

Effect of Cu concentration on the structural and optical properties of hierarchically porous Cu-doped ZnO nanostructures

Dea Uk Lee^a, Young Soo No^a, N. Sabari Arul^a, Tae Whan Kim^{a,*}, Hyoungkook Kim^b, Yongjin Bae^b and Jin Young Kim^c

^aDepartment of Electronics and Computer Engineering, Hanyang University, 222 Wangsimni-ro, Seongdong-gu, Seoul 133-791, Korea

^bDepartment of Electronic Engineering, Hanyang University, Seoul 133-791, Korea

^cDepartment of Electronic Material Engineering, Kwangwoon University, Seoul 139-701, Korea

Hierarchically porous Cu-doped ZnO nanostructures were formed on indium-tin-oxide (ITO)-coated glass substrates by using a template-free electrochemical deposition method. Field-emission scanning electron microscopy images showed that the density of the Cu-doped ZnO porous nanostructures increased with increasing Cu concentration. X-ray diffraction patterns showed that the lattice spacing of the (002) plane for the Cu-doped ZnO porous nanostructures decreased with increasing Cu concentration. Photoluminescence spectra for the Cu-doped ZnO porous nanostructures formed on the ITO-coated glass substrates showed that the dominant emission peak related to the band-to-band transitions shifted to a higher wavelength side with increasing Cu concentration.

PACS numbers: 82.45.Vp, 68.37.Hk, 61.10.-i

Key words: Cu-doped ZnO, Hierarchically porous nanostructures, Structural property, Optical property, Electrochemical deposition method.

Introduction

Zinc oxide (ZnO) has a direct wide band gap semiconductor (3.37 eV) and possesses excellent intrinsic properties, such as a large exciton binding energy of 60 meV at room temperature, high thermal stability, and environmental friendly material [1, 2]. The novel physical properties of the ZnO thin films and their superior chemical stability have stimulated promising applications in various optoelectronic devices, such as ultraviolet luminescence devices, light emitting diodes, photocatalysis, solar cells, gas sensors, and biosensors [3-7]. Doping in semiconductor thin films can tailor the electrical and optical properties of ZnO and widen its application area [7]. Among the various types of transition metal elements, the Cu dopants have attracted a great deal of interest because of their potential applications in electronic and optoelectronic devices [8]. Furthermore, Cu dopants act as an acceptor in ZnO crystals, which makes it an excellent candidate for forming p-type ZnO [9]. In addition, ZnO thin films grown by various techniques have been reported [10-14]. Among the various synthesis routes employed to grow ZnO nanostructures, the electrochemical deposition (ECD) method has been recognized as a potential technique because it is attractive, low cost, and easy to scale up to industrial level. Fur-

thermore, it facilitates in situ doping and decorating of the nanostructures [15]. Even though some investigations on the formation and physical properties of Cu-doped ZnO nanostructures have been carried out, studies concerning the effect of Cu concentration on the structural and optical properties of the Cu-doped ZnO hierarchically porous nanostructures have not been performed yet.

This paper reports data on the effect of Cu concentration on the structural and optical properties of Cu-doped ZnO hierarchically porous nanostructures formed on indium-tin-oxide (ITO) coated glass substrates by using the ECD method. Field-emission scanning electron microscopy (FESEM) and X-ray diffraction (XRD) measurements were performed to characterize the structural properties of the formed nominally un-doped and Cu-doped ZnO porous nanostructures. Photoluminescence (PL) measurements were performed to investigate the optical properties of the un-doped and Cu-doped ZnO hierarchically porous nanostructures.

Experimental Details

The Cu-doped ZnO hierarchically porous nanostructures used in this work were formed on ITO-coated glass substrates by using the ECD method. The resistivity of the ITO film was 17 Ω /square. The Cu-doped ZnO hierarchically porous nanostructures were formed by using the reduction of the dissolved molecular oxygen in zinc nitrate hexahydrate and various amounts of the Cu(II)

*Corresponding author:
Tel : +82-2-2220-0354
Fax: +82-2-2292-4135
E-mail: twk@hanyang.ac.kr

$(\text{CH}_3\text{COO})_2$ solutions. The shape and crystal structure of the Cu-doped ZnO nanostructures were controlled by varying the growth conditions of ECD. The ECD equipment used for the growth of Cu-doped ZnO nanostructures consisted of three-electrode electrochemical cells with an ITO cathode, acting as a working electrode. While an Ag/AgCl (3 M NaCl) electrode was used as the reference electrode, the platinum served as a counter electrode. $\text{Zn}(\text{NO}_3)_2 \cdot 6\text{H}_2\text{O}$ (1 mM) and KCl were dissolved in 250 ml of deionized water. The KCl (Sigma-Aldrich, 99.0-100.5%) acted as a supporting precursor [16], and the $\text{Zn}(\text{NO}_3)_2 \cdot 6\text{H}_2\text{O}$ (Sigma-Aldrich, 98.0%) acted as a Zn^{2+} precursor. Cu-doped ZnO porous nanostructures were formed by using a Cu concentration of 0, 3, or 5 wt%. The ZnO porous nanostructures were electrochemically deposited at 65 °C under a constant applied voltage of -0.9 V for 30 min.

FESEM measurements were performed by using a JSM-6330F scanning electron microscope. XRD measurements were carried out by using a Rigaku D/MAX-2500 diffractometer with Cu $K\alpha$ radiation, which was operated at a scanning speed of 5/min for a 2θ range between 20° and 70° . The X-ray tube voltage and the current were set to 40 kV and 100 mA, respectively. PL measurements were carried out using a 50 cm monochromator equipped with an RCA 31034 photomultiplier tube. The excitation source was the 325 nm line of a He-Cd laser, and the sample temperature was kept at 300 K.

Results and Discussion

Figure 1 shows the chronoamperograms as functions of the times recorded upon the growth of the Cu-doped ZnO porous nanostructures with a Cu concentration of (a) 0, (b) 3, or (c) 5 wt% deposited on ITO substrates. All chronoamperograms show an increase in the current at high temperature, and the reduction rate of the nitrate ions and the decomposition of zinc hydroxide

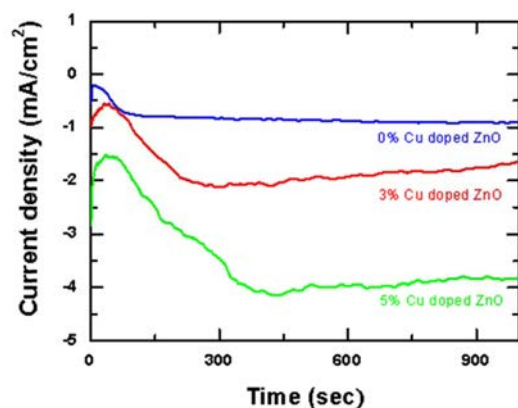


Fig. 1. Chronoamperograms as functions of times for Cu-doped ZnO porous nanostructures deposited on ITO substrates with a Cu concentration of (a) 0, (b) 3, or (c) 5 wt%.

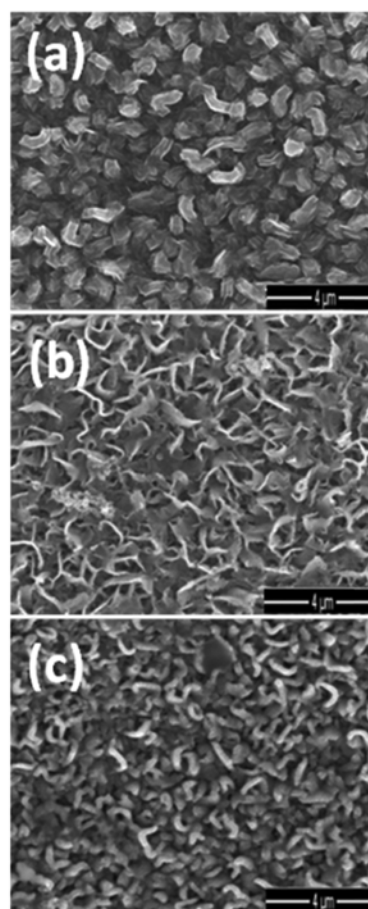


Fig. 2. Scanning electron microscopy images of the Cu-doped ZnO porous nanostructures deposited on ITO substrates with a Cu concentration of (a) 0, (b) 3, or (c) 5 wt%.

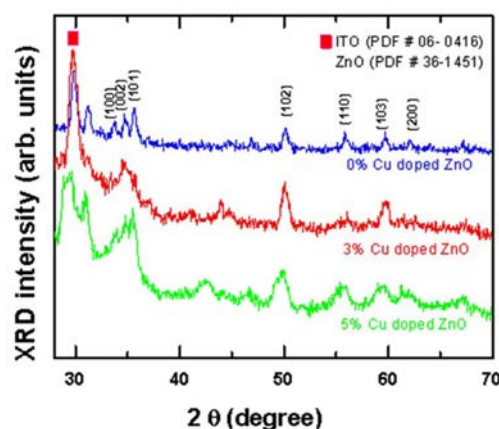


Fig. 3. X-ray diffraction curves of the Cu-doped ZnO porous nanostructures deposited on the indium-tin-oxide-coated glass substrates with a Cu concentration of (a) 0, (b) 3, or (c) 5 wt%.

are increased, resulting in an increase in the growth rate. The current for 0% Cu-doped ZnO nanostructures generated due to the reduction of molecular oxygen gradually increases with time and reaches a saturation level, as shown in Fig. 1. A steady state current density at a high concentration of Cu-doped ZnO was rapidly reached to -4 mA cm^{-2} . The current increase after 400

s may be due to an increase in the reduction rate of the nitrate ions occurring during deposition.

Figure 2 shows the FESEM images of Cu-doped ZnO hierarchically porous nanostructures grown with a Cu concentration of (a) 0, (b) 3, or (c) 5 wt%. The width of the nanostructures increased with increasing Cu concentration from 3 to 5%, as shown in Fig. 2. The doping of the Cu nanoparticles in ZnO nanostructures further provides a favourable condition for small deposits with rapid nucleation and growth, which occurs during electrodeposition with a high applied current or potential [17].

Figure 3 shows the XRD patterns of the Cu-doped ZnO porous nanostructures formed by using a Cu concentration of (a) 0, (b) 3, or (c) 5 wt%. The XRD patterns show that the Cu-doped ZnO porous nanostructures have polycrystalline hexagonal wurzite structures with lattice parameters of $a = 3.249 \text{ \AA}$ and $c = 5.206 \text{ \AA}$, which are in reasonable agreement with the literature values (JCPDS card, No. 36-1451). While no phase corresponding to Cu related compounds is observed in the XRD patterns, the peaks corresponding to the ITO substrate appear together with those related to the ZnO nanostructures. The broadening of the peak is clearly observed from the Cu-doped ZnO porous nanostructures.

The (002) peak position corresponding to the Cu-doped ZnO porous nanostructures shifts toward a larger degree in comparison with that related to the undoped ZnO porous nanostructures. The peak shift in a larger degree for the Cu-doped ZnO porous nanostructures is attributed to a decrease in the lattice spacing between the (002) planes resulting from the substitution of the Cu^{3+} into Zn^{2+} sites. The XRD results depict that the structure improves with increasing Cu doping concentration up to 5% and that the average crystallite size evidently decreases from 43 to 21 nm, which has been previously described in electrodeposited doped ZnO nanostructures [18].

The PL spectra of Cu-doped ZnO hierarchically porous nanostructures with a Cu concentration of 0, 3, or

5% are shown in Fig. 4. All of the spectra exhibit similar spectral features except for the PL intensity. The PL intensities of the characteristic peaks in the PL spectrum of 3 or 5% of Cu-doped ZnO porous nanostructures are smaller than that for 0% of Cu-doped ZnO nanostructures [19]. The decrease in the overall intensity of the PL spectrum is attributed to a decrease in the oxygen vacancies due to the Cu doping [20]. PL spectra exhibit two luminescence peaks at 2.2 and 3.2 eV, which are commonly observed in ZnO materials. The peak at 2.2 eV is attributed to the green PL usually identified as a trap luminescence related to an oxygen vacancy, and the peak 3.2 eV originates from the band-degree PL and is related to the electronic states extended in the nanocrystal volume. The PL intensity at 2.2 eV for 3% Cu-doped ZnO nanostructures is higher than that at 3.2 eV because the band to band transition is quenched by the defect states.

Summary and Conclusions

The effect of the Cu concentration on the structural and optical properties of the Cu-doped ZnO porous nanostructures formed on ITO-coated glass substrates by using an ECD method was investigated. FESEM images showed that the density of the Cu-doped ZnO porous nanostructures increased with increasing Cu concentration. XRD patterns showed that the average crystallite size for the Cu-doped ZnO porous nanostructures decreased with increasing Cu concentration. The PL spectrum showed that the overall intensity of the Cu-doped ZnO porous nanostructures decreased with an increase in a Cu concentration, which was attributed to a decrease in the oxygen vacancies resulting from the Cu doping. These results can help improve understanding of the effect of Cu concentration on the structural and optical properties of Cu-doped ZnO porous nanostructures for their potential applications in electronic and optoelectronic devices.

Acknowledgments

This research was supported by the Converging Research Center Program through the Ministry of Science, ICT and Future Planning, Korea (2013 K000202) and this research was supported by Leading Foreign Research Institute Recruitment Program through the National Research Foundation of Korea (NRF) funded by the Ministry of Education, Science and Technology (MEST) (No. 2013-044975). J.Y. Kim was supported by a Research Grant from Kwangwoon University in 2013.

References

1. C. Li, K. Hou, X. Yang, K. Qu, W. Lei, X. Zhang, B. Wang, and X. W. Sun, *Appl. Phys. Lett.* 93 (2008) 233508-

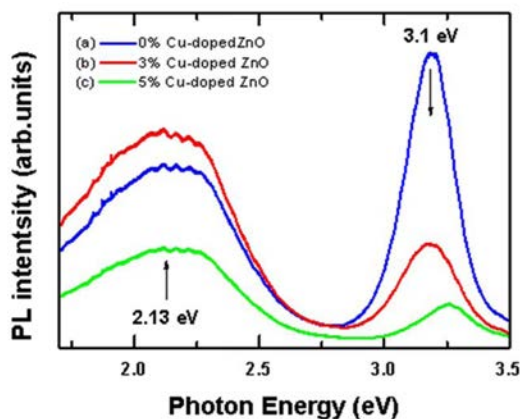


Fig. 4. Photoluminescence spectra for the Cu-doped ZnO porous nanostructures at room temperature with a Cu concentration of (a) 0, (b) 3, or (c) 5 wt%.

- 1-233508-3.
2. Q. Zhao, X. Y. Xu, X. F. Song, X. Z. Zhang, D. P. Yu, C. P. Li, and L. Guo, *Appl. Phys. Lett.* 88 (2006) 033102-1-033102-3.
3. F. Ye, X.-M. Cai, F.-P. Dai, S.-Y. Jing, D.-P. Zhang, P. Fan, and L.-J. Liu, *Phys. Status Solidi B* 249 (2012) 596-599.
4. J. H. Schon, A. Dodabalapur, Ch. Kloc, and B. Batlogg, *Science* 290 (2000) 963-965.
5. T. Soki, Y. Hatanaka, and D. C. Look, *Appl. Phys. Lett.* 76 (2000) 3257-3258.
6. A. Tsukazak, A. Ohtomo, T. Onuma, M. Ohtani, T. Makino, M. Sumiya, K. Ohtani, S. F. Chichibu, S. Fuke, Y. Segawa, H. Ohno, H. Koinuma, and M. Kawasaki, *Nat. Mater.* 4 (2005) 42-46.
7. H. Tsubomura, M. Matsumura, Y. Nomura, and T. Amamiya, *Nature* 261 (1976) 402-403.
8. Y. Chen, D. M. Bagnall, H. J. Ko, K. T. Park, K. Hiraga, Z. Zhu, and T. Tao, *J. Appl. Phys.* 84 (1998) 3912-3919.
9. Z. A. Khan and S. Ghosh, *Appl. Phys. Lett.* 99 (2011) 042504-1-042504-3.
10. O. Lupan, T. Pauporte, T. L. Bahers, B. Viana, and I. Ciofini, *Adv. Funct. Mater.* 18 (2011) 3564-3572.
11. W. I. Park, D. H. Kim, S. W. Jung, and G. C. Yi, *Appl. Phys. Lett.* 80 (2002) 4232-4234.
12. G. Shukla, *Appl. Phys. A* 97 (2009) 115-118.
13. J. Zuniga-Perez, A. Rahm, C. Czekalla, J. Lenzner, M. Lorenz, and M. Grundmann, *Nanotechnology* 18 (2007) 195303-1-195303-7.
14. [13] D. B. Buchholz, R. P. H. Chang, J. H. Song, and J. B. Ketterson, *Appl. Phys. Lett.* 87 (2005) 82504-1-82504-3.
15. D. Pradhan and K. T. Leung, *Langmuir* 24 (2008) 9707-9716.
16. D. Lincot, *Thin Solid Films* 487 (2005) 40-48.
17. S. P. Jiang, C. Q. Cui, and A. C. C. Tseung, *J. Electrochem. Soc.* 138 (1991) 3599-3605.
18. M. Schlesinger and M. Paunovic, *Modern electroplating*, 5th ed. (John Wiley & Sons, Inc., 2010).
19. M. Tortosa, M. Mollar, and B. Mari, *J. Cryst. Growth* 304 (2007) 97-102.
20. K. Borgohain and S. Mahamuni, *Semicond. Sci. Technol.* 13 (1998) 1154-1157.
21. H. Yang, Y. Xiao, K. Liu, and Q. Feng, *J. Am. Ceram. Soc.* 91 (2008) 1591-1596.